Fabrication of nanostar arrays by nanoimprint lithography

Teodor Veres[a)]
Industrial Materials Institute, National Research Council of Canada, 75 de Mortagne Blvd., Boucherville, Quebec J4B6Y4, Canada

Bo Cui
Industrial Materials Institute, National Research Council of Canada, 75 de Mortagne Blvd., Boucherville, Quebec J4B6Y4, Canada and Department of Electrical and Computer Engineering and Waterloo Institute for Nanotechnology (WIN), University of Waterloo, Waterloo, Ontario, N2L 3G1, Canada

Liviu Clime
Industrial Materials Institute, National Research Council of Canada, 75 de Mortagne Blvd., Boucherville, Quebec J4B6Y4, Canada

(Received 9 July 2010; accepted 27 September 2010; published 10 November 2010)

Using a low-cost and high-throughput process, this work demonstrates the fabrication of nanostar arrays over a large surface area, which would be an efficient substrate for surface enhanced Raman scattering applications. In the method, the nanostar is defined by the gap between four nanoholes "touching" each other. The two-dimensional periodic hole array was fabricated by nanoimprint lithography, and then the array pattern was transferred into a polymer layer sandwiched between two hard mask layers. Next, the holes in the polymer layer were enlarged by oxygen reactive ion etching (RIE) until its diameter was equal to the array period. The nanostar array was formed in the bottom hard layer after RIE, or it can be further transferred into a noble metal layer by lift-off steps. The authors fabricated a nanostar array with 200 nm tip-tip distance (equal to array period) and down to sub-10-nm apex and gap between adjacent stars. Numerical simulation confirmed the great enhancement of electromagnetic field near the star apexes. © *2010 American Vacuum Society.*
[DOI: 10.1116/1.3504890]

I. INTRODUCTION

Surface enhanced Raman scattering (SERS) is an effect where Raman scattering is enhanced tremendously (by up to 10^{12}) when molecules are attached to noble metal nanostructures. It is mainly due to localized surface plasmon resonance that leads to very high near field at the metal nanostructure surface that is analogous to the lightning rod effect, and to the fact that SERS enhancement is roughly proportional to the fourth power of the near field. Owing to its chemical specificity and label-free nature, SERS has found applications in detecting hazardous chemicals, explosives, chemical warfare agents, and biomolecules.[1,2] Ideal SERS substrates should offer a tunable resonance wavelength to match that of the laser excitation with high sensitivity and reproducibility. Whereas freestanding nanostructures (e.g., nanoparticles, nanowires, etc.) can be easily synthesized by chemical methods, it lacks tunability and reproducibility. The use of nanofabricated metallic structures can address these limitations. Nanostar array is ideal for SERS application. First, by varying the height/size of the nanostar, the resonance wavelength can be readily tuned over a broad range. Second, the sharp tips of the star result in extreme subwavelength focusing and thus greatly enhance the local electromagnetic field.[3] Finally, the small gaps between two adjacent stars further increase the local field by creating "hot spots."

Previously, nanostars have been synthesized chemically by using commercially available colloid (10 nm diameter gold colloid) as the seed.[4] However, the yield of a star-shaped structure was very low and the number of tips of each star was difficult to control. In addition, such method may not be applicable to materials other than Au. For better control and higher yield, nanolithography is preferred. It is straightforward to fabricate nanostars using electron beam lithography,[5] but with very low throughput and the sharpness of the tips may be limited by the back- and forward-scattering of electrons during exposure. By adding sub-5-nm bias structures near the tips to correct the proximity effect, feature sharpness could be greatly improved.[6] However, such a scheme would further reduce the throughput of electron beam lithography, since a smaller pixel (step size during exposure) is required. Nanosphere lithography (NSL) is a high-throughput and low-cost fabrication technique, and it has been employed to fabricate ordered three-tip nanostar (nanoprism) arrays into the gaps between three adjacent spheres.[7] However, any deviation from perfect arrangement in NSL leads to uncontrolled structures. This lack of control becomes even more evident for sub-500-nm spheres. In this article, we will report the fabrication of nanostar array by nanoimprint lithography (NIL) that is more flexible, with potentially better control than NSL.

II. FABRICATION AND RESULTS

Similar to NSL, the nanostar is defined by the gap between (four) adjacent nanoholes. As seen in Fig. 1, starting from a hole array, in which the diameter is much smaller than the array period, the nanostars are formed between adjacent

a)Electronic mail: teodor.veres@nrc.ca

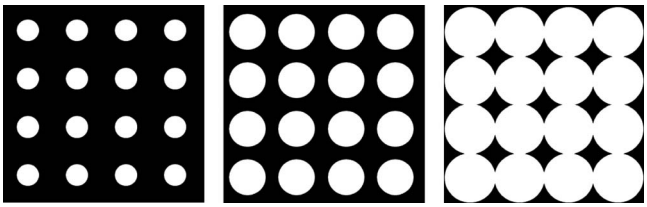

FIG. 1. Fabrication principle of nanostar array.

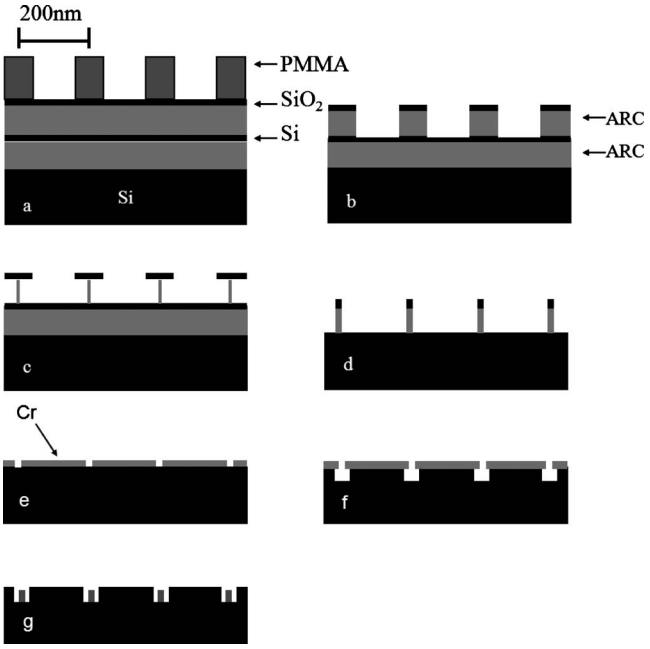

FIG. 2. Schematic process for the fabrication of nanostar array in ARC/Si [steps (a)–(d)] and Ti/Au [steps (e) and (f)]. (a) NIL into PMMA and etch away residual layer; (b) transfer pattern into oxide by CHF_3 RIE, then into ARC layer by O_2 RIE; (c) O_2 RIE to enlarge the hole in ARC; (d) remove oxide by HF, RIE Si using SF_6 gas, and then bottom ARC using O_2 gas; (e) evaporate and lift-off Cr by dissolving ARC; (f) RIE Si using SF_6 gas; and (g) lift-off Ti/Au by dissolving Cr using Cr–4S etchant.

holes when the hole is enlarged so that its diameter is equal to the array period. In principle, the holes in an imprint resist created directly by NIL can be enlarged by oxygen reactive ion etching (RIE), but it was found that such a process was hard to control because of the much faster etching rate along the vertical direction than the lateral direction. Consequently, we transferred the pattern into another polymer layer sandwiched between two hard mask layers, and then enlarged the holes in that polymer layer by RIE. This way, there was no etching along the vertical direction since the polymer layer was masked by the hard layer above. To prepare the substrate, a silicon wafer was cleaned using a mixture of $NH_4OH:H_2O_2:H_2O=1:1:5$ at 80 °C for 10 min, then a 160-nm-thick antireflection coating (ARC, XHRiC from Brewers Science) was spun and baked at 180 °C for 1 min to form a cross-linked polymer network. Si of 10 nm thickness was coated onto ARC by rf magnetron sputtering, followed by spin-coating the second layer ARC, onto which 10 nm SiO_2 was evaporated, thus forming a $Si/ARC/SiO_2$ sandwich structure for hole enlargement. Finally, 150 nm polymethyl methacrylate (PMMA) imprint resist was spin-coated and baked at 120 °C for 5 min.

The detailed fabrication steps for nanostar array in ARC/Si are shown in Figs. 2(a)–2(d). First, a hole array with 200 nm period and ~100 nm hole diameter was created into a PMMA resist by thermal NIL using a large area pillar array mold fabricated by two NILs at orthogonal directions using a grating mold fabricated by interference lithography. Although a circular hole would be preferred, other shapes, such as a square, will also result in nanostars after the fabrication process, as the hole enlargement process will make the square rounded. After NIL, the residual layer was etched by oxygen RIE. Second, the pattern was transferred into the thin (10 nm) SiO_2 layer using CHF_3 gas that etched similar amount of PMMA, then into ARC by oxygen RIE using the oxide as mask. Third, the holes were enlarged due to lateral etching during oxygen RIE. This step was the most critical, as too short an etch would not result in nanostar, whereas too long an etch would result in a blunt star. Fourth, after removing the top SiO_2 by diluted HF, the 10 nm Si was etched isotropically by SF_6 gas that etched negligible ARC. It is important to note that replacing the Si layer with a thin SiO_2 layer will not work because CHF_3 etching of oxide is anisotropic with significant passivation by fluorocarbon polymer, and thus, the area under the "shadow" by the top ARC layer will not be etched due to the lack of directional ion bombardment that helps remove the fluorocarbon polymer.[8] Once the Si was etched through, O_2 RIE was carried out to etch away the ARC layer below Si as well as the remaining ARC on top.

To form a SERS substrate, one can deposit Au or Ag using evaporation or sputtering on top of the ARC/Si nanostar array. However, we found that polymers (here ARC below Si) were susceptible to deformation when illuminated by focused laser beam during SERS measurement.[9] Therefore, we further transferred the star pattern into a noble metal on top of the silicon substrate. The process steps are shown in Figs. 2(e)–2(g). Onto the Si nanostar array, a Cr layer was first evaporated and lifted off by dissolving ARC using $NH_4OH:H_2O_2:H_2O=1:1:5$ at 80 °C for 10 min, resulting in a Cr nanodisk array on top of Si. Next, Si was etched isotropically using SF_6 gas to form an undercut profile below Cr. Finally, Ti/Au was evaporated and lifted off by Cr using Cr–4S etchant that etched Cr but not Ti and Au.

Figure 3 shows the scanning electron microscopy (SEM) images of the structure after a hole enlargement by oxygen RIE that corresponds to Fig. 2(c) as well as the completed nanostar array in Si. As expected, the lateral etching of ARC was faster at the lower part of the sandwich structure than the upper part. Here, the hole enlargement RIE was carried out using an Oxford PlasmaLab 80+ RIE System with a power of 100 W, a pressure of 100 mTorr, and an etching time of 5 min, which would etch away 650 nm ARC film. The lateral etch is ~40 nm, so the lateral etching rate was about 1/15 that of vertical. Because of the nonuniformity of the pillar

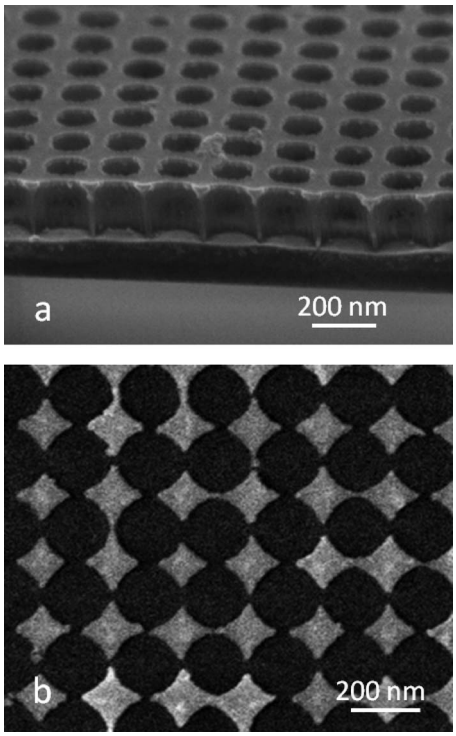

FIG. 3. SEM image of (a) enlarged holes in ARC (here the SiO_2 layer has been removed by HF) and (b) nanostar array in thin Si film on top of ARC.

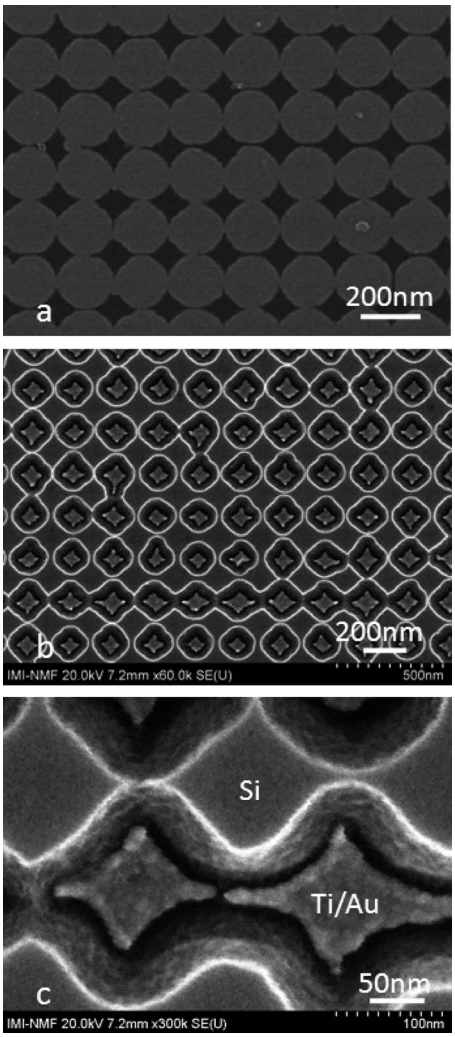

FIG. 4. SEM image of (a) Cr nanodisk array the diameter of which was equal to the array period, (b) 200 nm period nanostar array of 5 nm Ti/15 nm Au on silicon, and (c) zoom-in view of nanostars with sub-10-nm apex and gap between adjacent stars.

array pattern in the mold and process errors, the nanostar was found not perfect, with some stars connected and others blunt.

The Cr nanodisk array on Si after lift-off and the completed Ti/Au nanostar array are shown in Fig. 4. Due to additional process errors, the nanostars were less uniform than those shown in Fig. 3. Nonetheless, as shown in Fig. 4(c), the current technique is capable of producing nanostars with sub-10-nm apex and gap, which is well beyond those attained by NSL.

III. NUMERIAL SIMULATION

The discrete dipole approximation[10] (DDA) with a dipole grid length of 3 nm was used to calculate the near field and the extinction efficiency of the nanostar. The DDA algorithm is a powerful approach for computing the scattering of light by wavelength-scale particles of arbitrary structure and shape. The main idea behind DDA is to represent scattering particles by arrays of small dipoles located at the nodes of rectangular lattices and compute the electric moments of these dipoles induced by an incident electromagnetic wave. Its main advantage over other numerical algorithms, such as finite-difference time-domain, is that only the domain of interest (the scatters) has to be discretized, the polarizabilities at each node of the mesh being then used in order to compute the electric field at each point of the space. As shown in Fig. 5(a), the near field for a perfect freestanding nanostar with 200 nm tip-to-tip distance is greatly enhanced by nearly two orders of magnitude, and the electromagnetic near field is focused closer to the two apexes for the peak at 1000 nm than that at 600 nm. Here, there are two extinction peaks, which are consistent with the measured extinction spectrum of chemically synthesized nanostars in solution.[4] It would be interesting to see the extinction spectrum of a three-tip nanostar that results from NSL. We found that, unlike the four-tip nanostar, it has only one extinction peak at 1000 nm [see Fig. 5(b)]. For an array of four-tip nanostars, the near field would be further enhanced at the gap region between two stars. However, since (for 200 nm periodicity) the hot spot is ~15 and ~30 nm away from the end of the tip at $\lambda = 1000$ and 600 nm, respectively (which is due to the diminishing width near the end of the tip), it is expected that the near field enhancement at the gap would be less than that for the bowtie structure (two nanoprisms facing each other[11]) with sub-10-nm gap between the two prisms. Previously, the authors have fabricated a nanoprism array (where the prisms are along the same direction, rather than facing each other)

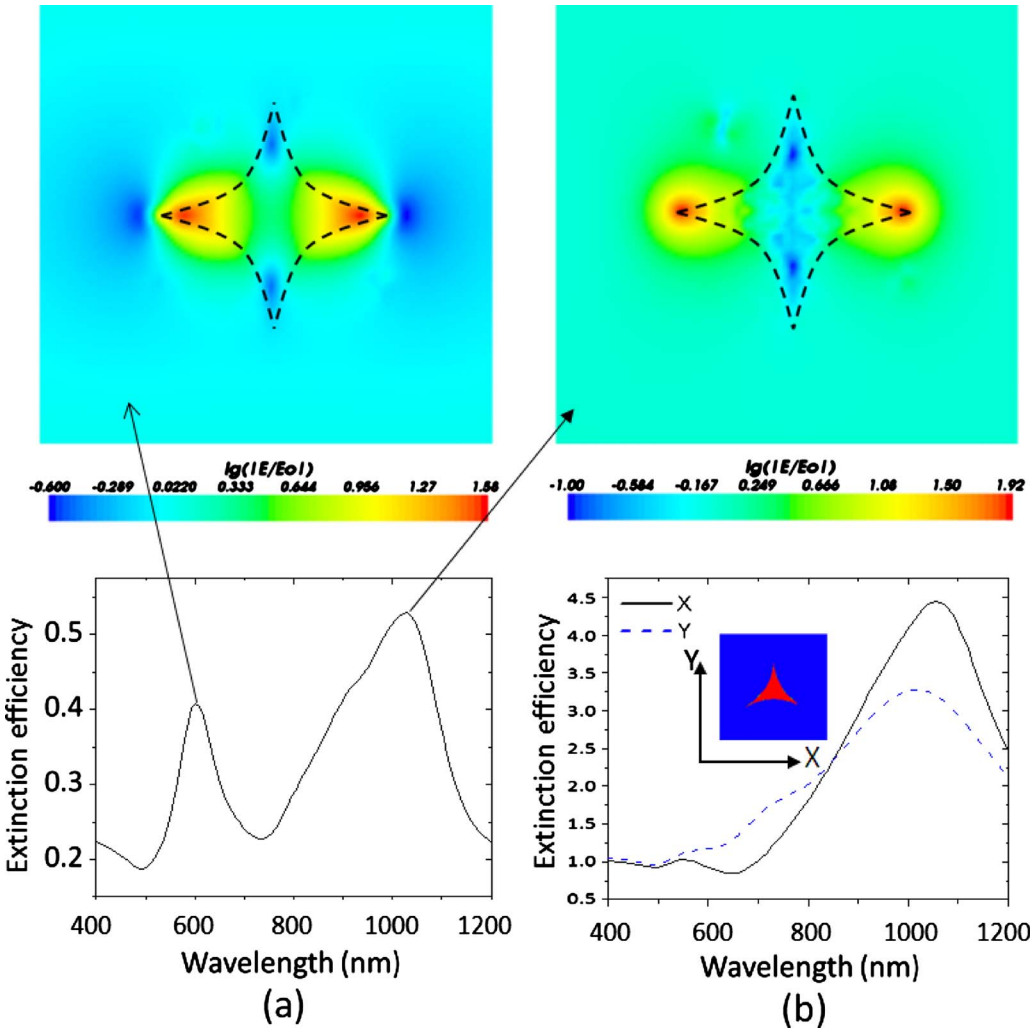

FIG. 5. (Color online) (a) Extinction spectrum and distribution of electromagnetic near field at the two resonance peaks (600 and 1000 nm) for a freestanding four-tip nanostar. (b) Extinction spectrum for a three-tip nanostar that shows only one peak at 1000 nm.

over a large surface area using nanoimprint lithography.[12] However, efficient and cost-effective fabrication of nanobowtie array remains a challenge.

IV. CONCLUSIONS

The fabrication of nanostars over a large area has been demonstrated using NIL, RIE, and metal evaporation and lift-off, which are all low-cost processes. The nanostar is defined by the gap between four holes touching each other. We created nanostar arrays with 200 nm period in noble metals. Numerical calculation using a DDA algorithm confirmed the great enhancement of the electromagnetic field near the sharp apexes. The current approach is orders more efficient than electron beam lithography and potentially more controllable than nanosphere lithography. It could find applications in biosensors and chemical sensors based on SERS detection.

[1]A. Campion and P. Kambhampati, Chem. Soc. Rev. **27**, 241 (1998).
[2]K. Kneipp, H. Kneipp, I. Itzkan, R. R. Dasari, and M. S. Feld, J. Phys.: Condens. Matter **14**, R597 (2002).
[3]K. Lesuffleur, L. K. S. Kumar, and R. Gordon, Phys. Rev. B **75**, 045423 (2007).
[4]C. L. Nehl, H. Liao, and J. H. Hafner, Nano Lett. **6**, 683 (2006).
[5]U. Huebner, R. Boucher, H. Schneidewind, D. Cialla, and J. Popp, Microelectron. Eng. **85**, 1792 (2008).
[6]L. E. Ocola, J. Vac. Sci. Technol. B **27**, 2569 (2009).
[7]T. R. Jensen, M. D. Malinsky, C. L. Haynes, and R. P. Van Duyne, J. Phys. Chem. B **104**, 10549 (2000).
[8]B. Cui and T. Veres, Microelectron. Eng. **84**, 1544 (2007).
[9]M. Geissler, K. Li, B. Cui, L. Clime, and T. Veres, J. Phys. Chem. C **113**, 17296 (2009).
[10]W.-H. Yang, G. C. Schatz, and R. P. Van Duyne, J. Chem. Phys. **103**, 869 (1995).
[11]P. J. Schuck, D. P. Fromm, A. Sundaramurthy, G. S. Kino, and W. E. Moerner, Phys. Rev. Lett. **94**, 017402 (2005).
[12]B. Cui, L. Clime, K. Li, and T. Veres, Nanotechnology **19**, 145302 (2008).